Atmospheric
Measurement
Techniques

External and internal cloud condensation nuclei (CCN) mixtures: controlled laboratory studies of varying mixing states

Diep Vu[1,2,a], Shaokai Gao[1,b], Tyler Berte[1,2], Mary Kacarab[1,2], Qi Yao[4], Kambiz Vafai[3], and Akua Asa-Awuku[1,2,4]

[1]Department of Chemical and Environmental Engineering, Bourns College of Engineering, University of California, Riverside, CA 92521, USA
[2]Bourns College of Engineering, Center for Environmental Research and Technology (CE-CERT), Riverside, CA 92507, USA
[3]Department of Mechanical Engineering, Bourns College of Engineering, University of California, Riverside, CA 92521, USA
[4]Department of Chemical and Biomolecular Engineering, A. James Clark School of Engineering, University of Maryland, College Park, MD 20742, USA
[a]currently at: Ford Motor Company, Research & Innovation Center, Dearborn, MI 48124, USA
[b]currently at: Phillips 66 Research Center, Research and Development, Bartlesville, OK 74004, USA

Correspondence: Akua Asa-Awuku (asaawuku@umd.edu)

Abstract. Changes in aerosol chemical mixtures modify cloud condensation nuclei (CCN) activity. Previous studies have developed CCN models and validated changes in external and internal mixing state with ambient field data. Here, we develop an experimental method to test and validate the CCN activation of known aerosol chemical composition with multicomponent mixtures and varying mixing states. CCN activation curves consisting of one or more activation points are presented. Specifically, simplified two-component systems of varying hygroscopicity were generated under internal, external, and transitional mixing conditions. κ-Köhler theory predictions were calculated for different organic and inorganic mixtures and compared to experimentally derived kappa values and respective mixing states. This work employs novel experimental methods to provide information on the shifts in CCN activation data due to external to internal particle mixing from controlled laboratory sources. Results show that activation curves consisting of single and double activation points are consistent with internal and external mixtures, respectively. In addition, the height of the plateau at the activation points is reflective of the externally mixed concentration in the mixture. The presence of a plateau indicates that CCN activation curves consisting of multiple inflection points are externally mixed aerosols of varying water-uptake properties. The plateau disappears when mixing is promoted in the flow tube. At the end of the flow tube experiment, the aerosols are internally mixed and the CCN activated fraction data can be fit with a single-sigmoid curve. The technique to mimic externally to internally mixed aerosol is applied to non-hygroscopic carbonaceous aerosol with organic and inorganic components. To our knowledge, this work is the first to show controlled CCN activation of mixed non-hygroscopic soot with hygroscopic material as the aerosol population transitions from externally to internally mixed states in laboratory conditions. Results confirm that CCN activation analysis methods used here and in ambient data sets are robust and may be used to infer the mixing state of complex aerosol compositions of unknown origin.

1 Introduction

Atmospheric cloud condensation nuclei (CCN) are comprised of complex mixtures of organic and inorganic compounds. The chemical and physical diversity present in complex mixtures can significantly complicate the quantification of aerosol–cloud interactions, thereby making it difficult to predict CCN activity (e.g., Riemer et al., 2019). In this work, we define mixtures and the aerosol mixing state as the chemical diversity across an aerosol distribution. Knowledge of

the mixing state and the chemical composition can greatly improve CCN predictions and has been the focus of several studies (e.g., but not limited to Bilde and Svenningsson, 2004; Abbatt et al., 2005; Henning et al., 2005; Svenningsson et al., 2006; King et al., 2007; Cubison et al., 2008; Kuwata and Kondo, 2008; Zaveri et al., 2010; Su et al., 2010; Wang et al., 2010; Spracklen et al., 2011; Ervens et al., 2010; Asa-Awuku et al., 2011; Lance et al., 2013; Liu et al., 2013; Jurányi et al., 2013; Paramonov et al., 2013; Padró et al., 2012; Moore et al., 2012; Meng et al., 2014; Bhattu and Tripathi, 2015; Almeida et al., 2014; Schill et al., 2015; Crosbie et al., 2015; Che et al., 2016; Ching et al., 2016; Mallet et al., 2017; Sánchez Gácita et al., 2017; Cai et al., 2018; Schmale et al., 2018; Mahish et al., 2018; Kim et al., 2018; Chen et al., 2019; Stevens and Dastoor, 2019).

It is well accepted that the water content and the point of activation is dependent on more factors than just the supersaturation and dry diameter for CCN active aerosols (Dusek et al., 2006; Petters and Kreidenweis, 2007). The droplet growth and activation of slightly soluble organics can be modified when internally mixed with inorganic salts that readily deliquesce (Cruz and Pandis, 1998; Padró et al., 2002; Svenningsson et al., 2006). Although inorganic salts are well characterized, the quantification of CCN activity is complicated when they are internally mixed with a complex organic. Consequently, simple mixing rules may no longer be appropriate. It has been observed that mixed aerosols can activate at lower supersaturations than their bulk constituents and organic compounds that may not traditionally be considered water soluble may aid in the formation of a cloud droplet by acting as a surfactant, depressing surface tension, or simply by contributing mass (Cruz et al., 1998; Padró et al., 2007; Svenningsson et al., 2006). In addition, when there is a sufficiently large enough fraction of salt, the slightly soluble core can dissolve before activation, thus lowering the required supersaturation (Sullivan et al., 2009). Thus, the mixing state and extent of mixing can substantially influence CCN activity.

To help minimize the complexity in characterizing aerosol hygroscopic and CCN activation properties, CCN data analysis has traditionally been simplified by assuming that (i) the aerosols share a similar or uniform hygroscopicity over a particle size distribution, (ii) the CCN particle size can be described by the electrical mobility diameter, (iii) CCN consist of few multiply charged aerosols, and (iv) all CCN active aerosols readily dissolve at activation. As a result, a singular sigmoidal fit is commonly applied over the entire CCN activation. However, this method of analysis may not be fully representative of the heterogeneous mixing state occasionally present in the aerosol sample. Thus a CCN mixture refers to the diversity of activated aerosols in the particle population (not the property of an individual particle; Winkler, 1973; Riemer et al., 2019).

Previous studies have addressed aerosols with singular or internally mixed binary chemical species (e.g., but not lim-

ited to Bilde et al., 2004; Broekhuizen et al., 2004; Petters and Kreidenweis, 2007; Shulman et al., 1996; Sullivan et al., 2009). However, ambient measurements indicate complex aerosol populations consisting of both external and internal mixtures (e.g., but not limited to Ervens et al., 2007; Lance et al., 2013; Moore et al., 2012; Padró et al., 2012). By accounting for the mixing states and extent of mixing in field data sets, CCN concentration predictions can be greatly improved (e.g but not limited to Padró et al., 2012; Wex et al., 2010; Su et al., 2010; Kuwata and Kondo, 2008). However, dynamic changes in particle mixing states have not been reproduced in the laboratory and subsequent treatment of CCN measurement and analysis has not been readily studied in depth under controlled laboratory conditions.

In this work, we seek to improve the experimental CCN activation analysis techniques of complex mixtures by investigating the influence of mixing state on activation curves with known aerosol composition. Theoretical postulations have already been developed and applied to ambient data sets (e.g., but not limited to Su et al., 2010; Padró et al., 2012; Bhattu et al., 2016) but never before has a systematic laboratory experiment controlled and validated the extent of particle heterogeneity for CCN activation. To understand the impact of mixing state on CCN activation, simplified two-component mixtures of known compounds with varying hygroscopicities are created under internal, external, and in-between (transition) mixing conditions. In addition, black-carbon-containing particles (BC) and BC mixing state data are presented. BC is renowned for its direct radiative effects yet little is known experimentally about the contributions of BC mixtures to aerosol–cloud interactions at varied mixing states. Previous work investigating the contribution of BC to aerosol–cloud interactions at various mixing states has been studied (e.g., but not limited to Bond et al., 2013 and references therein, Lammel and Novakov, 1995; Novakov and Corrigan, 1996; Weingartner et al., 1997; Dusek et al., 2006; Kuwata and Kondo, 2008; Koehler et al., 2009; McMeeking et al., 2011; Liu et al., 2013; Rojas et al., 2015). However, many of the already published works are ambient field studies; less work has been studied under controlled laboratory settings. Here, the CCN activation and hygroscopic properties of soot mixed with atmospherically relevant constituents of varying hygroscopicity are investigated under laboratory controlled conditions. This work provides evidence on the differences between inorganic, slightly soluble, and insoluble externally and internally mixed compositions for the uptake of water, and subsequent CCN activity.

2 Experimental methods

2.1 Aerosol composition and sources

The CCN activity of two-component aerosol mixtures under internal, external, and combinations of mixing states

is explored in this study. The components include very hygroscopic (inorganics), hygroscopic (organic acids), and non-hygroscopic (black carbon, BC). For known chemical compositions, a Collison-type atomizer generated singular-component solutions of ammonium sulfate ($(NH_4)_2SO_4$, Acros 99.5 %), sodium chloride, (NaCl, Acros 99+ %), and succinic acid ($C_4H_6O_4$, Acros 99 %) and subsequent internal mixture combinations as described in the sections Aerosol mixing states and Modified mixing states: external to internal. Succinic acid, classified as a slightly soluble dicarboxylic acid, (18) $(NH_4)_2SO_4$, and NaCl are all relevant model atmospheric compounds with varying degrees of solubility and hygroscopicity. All atomized solutions were prepared using Millipore© DI water (18 mΩ, TOC $\leq$ 5 ppb). Atomized wet droplets were dried with silica gel diffusion dryer (as commonly practiced). In addition, we employ a heated column before the diffusion dryer to facilitate the evaporation of water from the wet particles. The implications of the use or absence of a heated column are discussed in the results below.

An AVL particle generator (APG), which houses a mini combustion aerosol standard soot generator (miniCAST 6203C, Jing Ltd.), was used to generate carbonaceous aerosols. The APG consists of a propane burner followed by a volatile particle remover. The burner was operated at 400 °C with a propane and air flow rate of 15 mL min^{-1} and 1.0 L min^{-1}, respectively. The miniCAST utilized in the APG has been well characterized in previous work (e.g., Pinho et al., 2008; Seong and Boehman, 2012; Mamakos et al., 2013; Maricq and Matti Maricq, 2014; Durdina et al., 2016; Moore et al., 2014). The soot formed is a mixture of black and oxidized carbon (Moore et al., 2014). The aerosol structures generated by the APG likely consisted of fractal-like agglomerates of nonspherical particles (Moore et al., 2014; Durdina et al., 2016). APG combustion aerosols are mixed with inorganic and slightly soluble succinic acid, and CCN activity is subsequently measured at different supersaturations.

2.2 Aerosol mixing methods

Mixing compounds in solution can readily form internal mixtures of aerosol (Gibson et al., 2007; Hameri et al., 2002). Solution mixtures of a highly hygroscopic compound, NaCl, and a slightly hygroscopic compound, succinic acid, are shown. Five aqueous solutions of succinic acid and NaCl with molar ratios of 100 : 0, 87 : 13, 69 : 31, 43 : 57, and 0 : 100 were aerosolized using a single atomizer, passed through a heated column, dried, and sampled directly into a scanning mobility particle sizer (SMPS) and CCN counter (CCNC). Instrument specifications are discussed in Sect. 2.3.

External mixtures were formed via two methods. The first and simplest method required two sufficiently dry aerosol streams to mix. Two aerosol streams were joined via a Swagelok® Tee connector. External mixtures were also
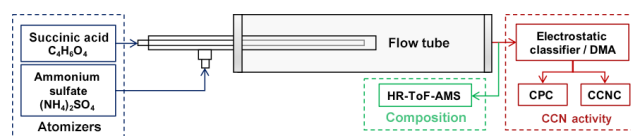

Figure 1. External and internal mixtures with gradual mixing in flow tube.

formed in a flow tube mixing apparatus. As conditions (e.g., but not limited to, residence time, temperature, pressure, relative humidity) change in a flow tube, it is assumed that the external mixture may transition into an internally mixed aerosol system. A flow tube mixing apparatus was constructed to test this assumption and modify the extent of mixing of multiple components (Figs. 1 and 2).

This work shows changes in CCN experimental data and analysis as a result of changes in the extent of mixing. Results of the CCN activation are presented in the section Modified mixing: external to internal mixing in the aerosol flow tube. A brief description of the flow tube is provided here. The first aerosol stream is introduced into the flow tube by a 1/4 in. stainless steel (SS) tube. The second aerosol stream is also introduced by a 1/4 in. SS tube, but is expanded to an outer concentric 1/3 in. SS tube using a SS Swagelok tee connection. The two aerosol flows are initially mixed together at the exit of the 1/4 in. tube and aerosol mixes within the 1/3 in. SS tube for an additional 12 in. before entering the quartz tube where it continues to mix. In this study, the pressure and temperature of the flow tube are maintained at ambient conditions. The extent of mixing in the flow tube mixer has been modeled by computational fluid dynamics simulation (CFD – COMSOL) to test and improve the aerosol mixing capabilities of the flow tube mixer (Fig. S1). The focus of this work is not the mixing apparatus but the CCN behavior that results from changes in the extent of mixing. It is noted that particle losses likely occur within the flow tube system but do not affect the intrinsic aerosol and CCN properties (activated fractions) presented here.

2.3 CCN activity and chemical composition: measurements and instrumentation

CCN activation is measured with particle sizing and counting instrumentation in parallel with CCN counting instrumentation. This technique is widespread and has been used in numerous publications (e.g., but not limited to Moore et al., 2010; Padró et al., 2012). The development of a single continuous-flow thermal gradient diffusion column CCN counter, CCNC (Droplet Measurement Technologies, Inc.) has provided rapid ($\sim$ 1 Hz) and robust CCN data (Lance et al., 2013; Roberts and Nenes, 2005). Aerosols with a S_c lower than the supersaturation in the column activate and form droplets. These droplets are detected and counted using an optical particle counter at the exit of the column.
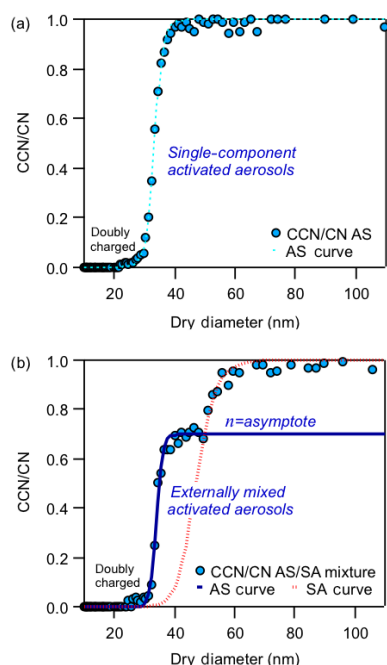
Figure 2. Example of a charge-corrected **(a)** single-component activation curve and **(b)** a multiple activation curve from an externally mixed/heterogeneous system. The asymptote, η, varies in height and length with the presence of mixed components and their respective hygroscopicities.

A TSI 3080 electrostatic classifier selects and measures aerosol size distributions. Polydisperse aerosol streams are passed through a bipolar krypton-85 charger and then through a differential mobility analyzer (DMA), where the aerosols are sized according to electrical mobility with a sheath-to-aerosol flow ratio of 10 : 1. The monodispersed flow is then split to a condensation particle counter (CPC) and a CCN counter. CN concentrations were measured with a CPC (TSI 3772, TSI 3776).

The CCNC is operated at 0.5 lpm with a sheath-to-aerosol flow ratio of 10 : 1 and is calibrated with $(NH_4)_2SO_4$ to determine the instrument supersaturation (Rose et al., 2008). Operating the CCN in parallel with the CPC allows for the simultaneous measurements of the total CN and CCN of the monodispersed aerosols. By operating the DMA in scanning voltage mode and maintaining a constant column supersaturation, the CCN / CN, or activation ratio, as a function of dry diameter can be obtained for a given supersaturation. These size-resolved CCN distributions obtained through scanning mobility CCN analysis (SMCA) produce CCN activation curves and CCN / CN ratio as a function of particle mobility diameter (Moore et al., 2010). SMCA produces high-resolution CCN activation data near the 50 % efficiency critical diameter every $\sim$ 2 min.

An Aerodyne high-resolution time-of-flight aerosol mass spectrometer (HR-ToF-AMS) measured the non-refractory bulk composition (DeCarlo et al., 2006). The HR-ToF-AMS

was operated in V-mode to track the concentration and vacuum aerodynamic diameter as the aerosol fractions were modified.

3 CCN analytical method

CCN data analysis of single-component aerosols, such as ammonium sulfate (AS), are well characterized. The activation of a single known component yields a simple sigmoidal activation curve and is often used for instrument calibration (Fig. 2a). However ambient aerosols generally exist as complex mixtures of organic and inorganic species. CCN data sets from ambient and chamber studies, which consist of these aerosol mixtures, may not show a single-sigmoid activation curve but instead can exhibit multiple activation curves not associated with doubly charged particles (Fig. 2b).

Sigmoidal fits are applied to the CCN / CN as a function of dry activation diameters for the multicomponent aerosols. Externally mixed aerosol fractions in activation curves have been previously observed in ambient studies by Lance et al. (2013), Moore et al. (2012), and Bougiatioti et al. (2011). For those studies, E was defined as the hygroscopic fraction, and $1 - E$ the non-hygroscopic mixed fraction. For this study the first curve is similarly defined as the hygroscopic externally mixed fraction (EMF) with an asymptote, or plateau, of η. The dependence of η varies with the presence of mixed components and their respective hygroscopicities. Thus we evaluate η for controlled compositions and compare how representative they are of the known fractions of mixtures.

A sigmoidal fit through the EMF determines the particle dry diameter of the more hygroscopic species. A second sigmoidal fit is applied to the second activation curve. An example is shown in Fig. 2b for an external mixture of AS and succinic acid (SA). A sigmoid is fit for the more hygroscopic species, AS, and then a second for the less hygroscopic species, SA. The activation diameters are consistent with those expected for the two compounds and agree with Köhler predicted activation values for AS and SA. Doubly charged aerosols are indicated in Fig. 2 and are a negligible contribution to the activation curves.

The supersaturation and critical dry diameter are related via the single parameter hygroscopicity, κ, to describe the CCN activity and to determine the effect of mixing states of multiple components on the supersaturated hygroscopic properties of aerosols. Using the generalized κ-Köhler equations presented by Petters and Kreidenweis (2007, 2008), droplet growth in the supersaturated regimes for a selected dry diameter can be modeled for an aerosol where the entire particle diameter dissolves at activation.

$$\ln S_c = \left(\frac{4A^3 \rho_w M_s}{27 v \rho_s M_w D_d^3} \right)^{1/2}, \quad \text{where } A = \frac{4\sigma_{s/a} M_w}{RT \rho_w} \tag{1}$$

$$\kappa = \frac{4A^3}{27D_d^3 \ln^2 S_c} \qquad (2)$$

$\sigma_{s/a}$ is the surface tension, M_w is the molecular weight of water, R is the universal gas constant, T is the temperature at activation, and ρ_w is the density of water. Surface tension and density of water were calculated according to temperature-dependent parameterizations presented by Seinfeld and Pandis (1998) and Pruppacher and Klett (1997). The surface tension of the solution is assumed to be that of pure water. Traditional Köhler theory is known to work reasonably well for inorganic salts and slightly soluble and hygroscopic organics like succinic acid.

4 Results and discussion

4.1 Internal mixtures

Aerosolized internally mixed solutions exhibit single CCN activation curves for all five compositions of succinic acid and NaCl solutions (Fig. 3a). The activation curve is similar to that of ammonium sulfate in Fig. 2a. Multiply charged particles contribute less than 10 % to the activated fraction and are assumed to be negligible. A sigmoid that plateaus near one can be applied to describe the CCN activation. As the internal mixture salt fraction increased at a given supersaturation, the single curve was maintained and shifted towards a lower activation diameter, indicative of and consistent with more hygroscopic aerosol. The shifting of the CCN activation sigmoid (left and right) is also expected of internally mixed particles formed via the coagulation of separate particle distributions (Farmer et al., 2015). Using the simple mixing rule, a multicomponent hygroscopicity parameter can be theoretically applied based on the expected kappa values for each individual component hygroscopicity (κ_i), and the volume fraction of each component (ε_i) (Petters and Kreidenweis (2007).

$$\kappa = \sum_i \varepsilon_i \kappa_i \qquad (3)$$

Equation (3) was applied for each mixture. κ was calculated and compared to the experimental values (Fig. 3b). These internal mixtures do not strongly follow the simple mixing rule for every mixture and are consistent with the previous work of Shulman et al. (1996) and Padró et al. (2007), who showed that slightly soluble compounds internally mixed with salts resulted in surface tension depression and thus a lower required critical supersaturation. As previously published, accounting for organic surface tension depression could improve kappa-hygroscopicity calculations for internal mixtures. Regardless of surface tension omissions, the single-sigmoid experimental data set is within 20 % of theoretical agreement and indicative of a single-component or homogeneous internally mixed aerosol population.
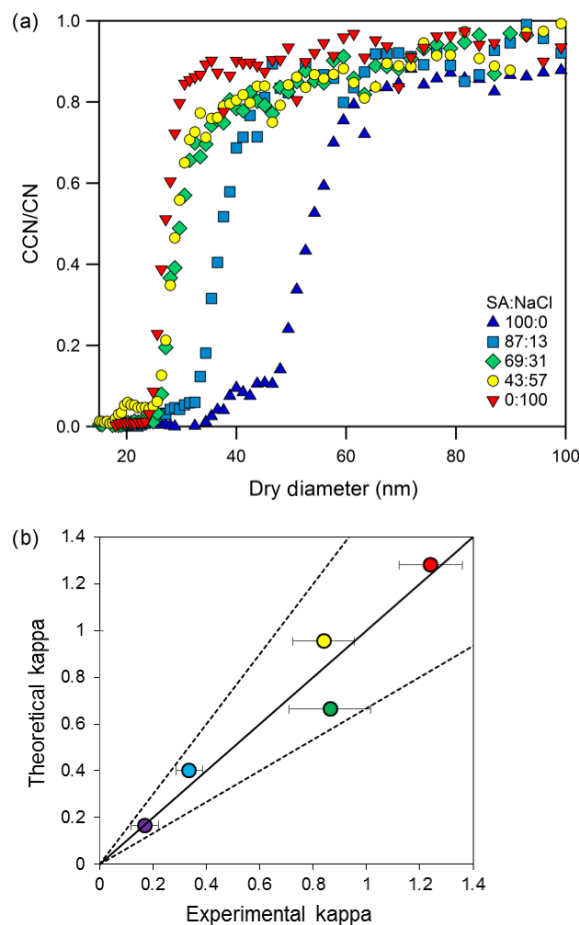
Figure 3. (a) Activation curves for two-component internal mixtures of NaCl and succinic acid (SA) at SS 0.72 %. Doubly charged aerosols are present but are all below 0.1 and negligible. **(b)** Internally mixed aerosols. Multicomponent hygroscopicity parameter predictions vs. experimentally derived kappa values. Dashed lines indicate 50 % uncertainty (1 : 1.5 and 1.5 : 1). Data are within 20 % uncertainty of the 1 : 1 line.

4.2 External to internal aerosol mixing results

Individual single-component aqueous solutions of ammonium sulfate (AS), $(NH_4)_2SO_4$, and succinic acid (SA) were aerosolized and dried with an active heated column and silica gel diffusion dryer to produce external mixtures. Data sets yielding multiple activation curves consistent with external mixing were successfully created by (i) mixing aerosol streams and (ii) injecting SA and AS compounds in the flow tube. For this paper, we show externally mixed data generated from the use of the mixing flow tube. The direct mixing produces the same externally mixed CCN results (not shown). By using aerosols consisting of compounds of significantly different hygroscopicities, and thus different activation diameters, distinct double plateaus for CCN activation can be observed for external mixtures (Fig. 2b). At particle mobility diameters between $\sim$ 35 and 45 nm there is an

asymptote, $\eta \sim 0.6$ (Fig. 4a, b, and c). It is noted that heated succinic acid particles can evaporate during aerosol generation before CCN measurement; the asymptote in Fig. 4 is an indication that multiple components are present in the total aerosol distribution. The activation curves were characteristic of AS and SA, and the measured activation diameters agreed well with Köhler theory and the single-parameter (κ) thermodynamic predictions of droplet activation (Fig. 4a). The external mixture was maintained for an hour as indicated by the separate and stable activation diameters derived from multiple-sigmoid analysis. For more than two-component externally mixed particle distributions, more than two plateaus will be observed. For example, the work of Schill et al. (2015) shows multiple plateaus for a five-component external mixture mimic of ocean spray CCN. If one considers a limiting case of infinite components with distinct varying degrees of hygroscopicity, then the activation curve will be monotonic below 1 and may appear to be representative of an internal mixture; the CCN activation curve will approach the shape of a shallow sigmoidal slope (however not as steep or instantaneous as the ideal step function).

A total of 1 h after initial injection into the flow tube, the active heating column was turned off. It should be noted that atomized aerosol continued to be dried through the silica gel diffusion dryers, as is commonly done. The relative humidity after the dryer in both cases is small ($< 20\%$) and thus the activation diameters of very hygroscopic AS calibration aerosol are not affected with or without active heating (Fig. S2). However, as soon as active heating was turned off, particles in the mixing flow tube became more mixed (Fig. 4). Thus, it is likely that minute amounts of aerosol water promoted internal mixing and shifted aerosol mixing from external to internal in the mixing flow tube system.

CCN activation curves for the two compounds remained distinct and separate until internal mixing conditions dominated and the multiple CCN activation curves converged into a single curve (Fig. 4b and c). Results suggest aerosol water plays a significant factor in mixing and CCN activation. This is consistent with previous work that indicates that the presence of water led to lowered aerosol viscosity and increased diffusivity (Ye et al., 2016). The wetted aerosols can come in contact through diffusion and coalesce to form an internally mixed aerosol. The apparent kappa values from fitting the two individual activation curves for the external part of the mixing experiment and subsequent internal mixing are shown in Fig. 4a.

To help track the change in organic/inorganic fractions during the transition from external to internal, the mixed aerosols were analyzed with a high-resolution time-of-flight mass spectrometer (HR-ToF-AMS) to provide mass fraction information. The mass size distribution was integrated and normalized for each compound per scan according to the total mass that was measured. The mass size distribution was then converted to number size distribution and the diameters were converted from aerodynamic diameter to electrical
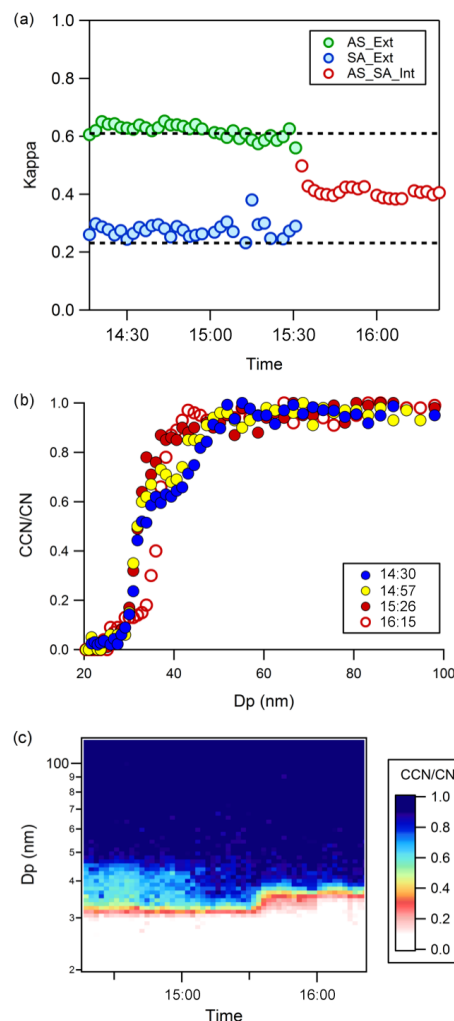
Figure 4. External to internal mixtures of a slightly soluble organic aerosol, succinic acid (SA), and inorganic ammonium sulfate (AS) aerosol. The CCNC was operated at a single S_c of 0.8 %. Closed symbols are externally mixed. Open symbols are internally mixed. **(a)** The apparent kappa values derived from externally mixed multiple-sigmoid activation data before active heating is turned off (at approximately 15:30 PDT, Pacific daylight time, for all times in the paper) and single-sigmoid activation curves (after 15:30) are shown. The two dotted lines indicate the theoretically derived kappa values for succinic acid, $\kappa = 0.23$, and ammonium sulfate, $\kappa = 0.61$. **(b)** CCN activation curves exhibit external (with active heating before 15:30) and then transitioning external to internal mixing (after 15:30) **(c)** CCN / CN vs. dry mobility diameter data as a function of time. The asymptote, η, disappears by the end of the experiment.

mobility diameter. Then for each supersaturation and fraction, the EMF was calculated between the two respective activation diameters and correlated to the EMF that was determined from SMCA to determine the plateau height (η).

AS fractions measured by the AMS are consistent with the changes in SMCA-derived η where increases in AS mass
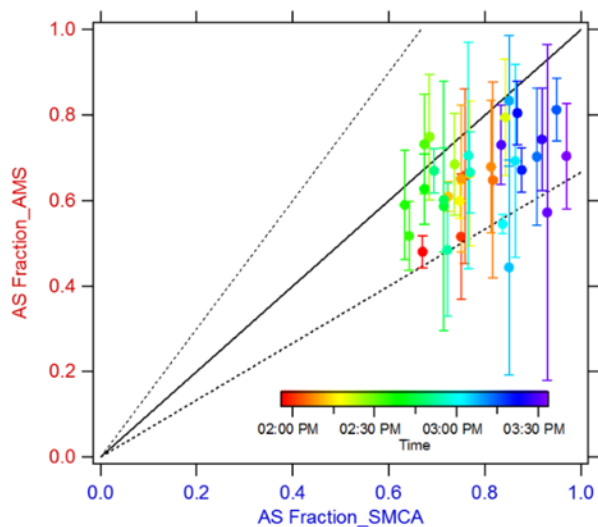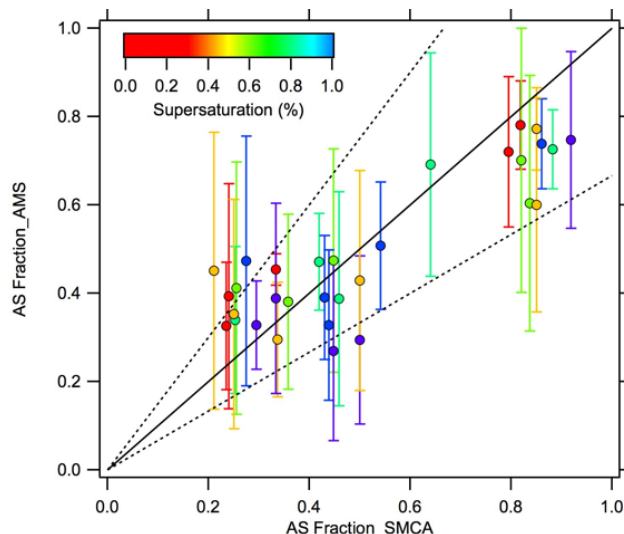
Figure 5. Plateau heights derived from AMS data vs. SMCA. Single CCNC supersaturation. Dashed lines indicate 50 % uncertainty (1 : 1.5 and 1.5 : 1).
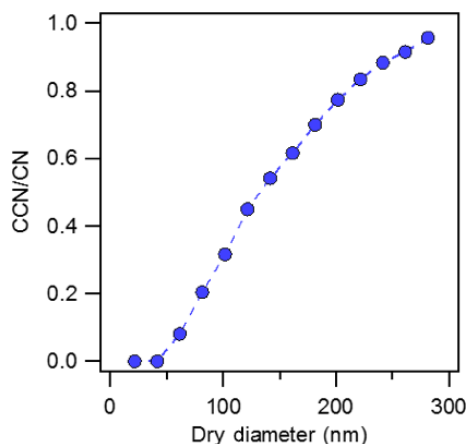

Figure 6. Modifying activation diameters. Plateau heights derived from AMS data vs. SMCA for CCNC supersaturation from 0.2 % to 1.2 %. Dashed lines indicate 50 % uncertainty (1 : 1.5 and 1.5 : 1).

fraction increase η. However, the AMS-derived AS fractions are slightly lower compared to SMCA (Fig. 5), indicating potential influence on η from other factors. Previous work has shown the presence of highly soluble materials (like AS) can promote CCN activity of organic-dominated systems (Asa-Awuku et al., 2011; Fofie et al., 2017). A second flow tube experiment was conducted to test the effect of differing concentrations on plateau heights. The detection efficiency for particles with smaller sizes in the AMS (<50 nm) can effect the AS fraction. Thus, the CCNC supersaturation was modified from 0.2 % to 1.2 % to test the effect of activation diameter on closure (Fig. 6). Results show good agreement and are within 50 % of predictions. Results with distinct CCN activation plateaus, especially of two to three distinct hygroscopicities, may be useful for estimating aerosol chemical fractions when other instruments with lower size resolution are not readily available.

4.3 External and internal mixtures of combustion aerosol

Combustion aerosol or soot can form external and internal complex aerosol mixtures. Soot is considered insoluble but wettable (e.g., but not limited to Lammel and Novakov, 1995; Moore et al., 2014) and the contributions of black-carbon-containing particles to aerosol–cloud interactions at varied mixing states are not well known or understood (Lammel and Novakov, 1995; Novakov and Corrigan, 1996; Weingartner et al., 1997; Dusek et al., 2006; Kuwata and Kondo, 2008; Koehler et al., 2009; Bond et al., 2013; McMeeking et al., 2011; Liu et al., 2013; Rojas et al., 2015). Thus, the ability of black carbon to mix with inorganic and organic compounds

and to observe the extent of mixing as they activate as CCN is of great interest.

Prior to investigating the impact of mixing fresh combustion emissions with inorganic and organic aerosols, the CCN activation spectra of soot were measured using combustion aerosol generated from the APG. The aerosol is likely composed of black carbon and oxidized carbonaceous material (Moore et al., 2014; Durdina et al., 2016). Thus we also refer to carbonaceous aerosol as black carbon mixtures (simply, BC mixtures). The CCN-activated fraction data from soot were fit to a singular sigmoidal curve (Fig. 7). There are no plateaus in the activation curve and the single-sigmoid fit indicates that the aerosol generated is a homogenous internal mixture. Combustion aerosol activated at a mobility diameter of 133 nm at 2.2 % supersaturation. The apparent hygroscopicity of combustion aerosol was $\kappa = 0.001$, and is consistent with the order of magnitude and kappa values reported for fresh combustion aerosol from diesel engine sources (Fig. 7) (Vu et al., 2015; Moore et al., 2014). It is noted that the apparent hygroscopicity is defined by the electrical mobility diameter that assumes particles are spherical.

Next, the influence of modifying externally mixed hygroscopic aerosol fractions with non-hygroscopic BC mixtures was observed. Soot was externally mixed with various concentrations of AS and NaCl in two separate experiments. For each BC mixture, combustion aerosol was introduced to the flow tube and atomized inorganic and organic aerosol (dried with a heated column and silica gel diffusion dryers) was injected. The concentration of inorganic aerosol in the flow tube was slowly increased to modify the contribution of soluble material. The CCN counter supersaturation was
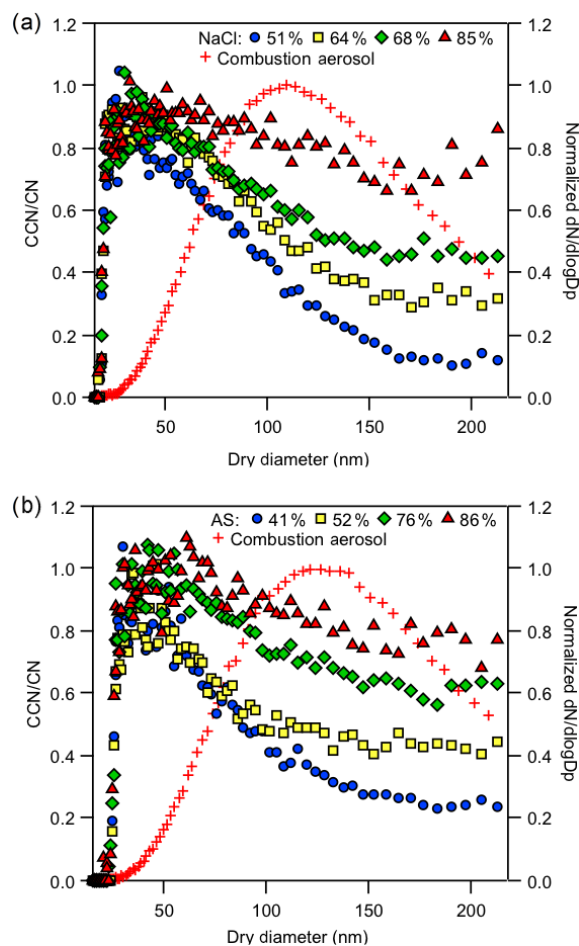
Figure 7. Combustion aerosol activation curve (SS 2.2 %, $d_{p,50} = 133\,nm$, $\kappa = 0.001$).

Figure 8. Combustion aerosols externally mixed with inorganics. **(a)** NaCl externally mixed with concentrations modified from 51 % to 85 % over the course of 60 min. **(b)** AS externally mixed with concentrations from 41 % to 86 % over the course of 75 min. Cross symbols represent the initial size distribution of the combustion aerosol.

decreased to 1.1 % to observe the impact of the more hygroscopic compounds in the BC mixture.

Figure 8 shows the CCN activation of external mixtures of BC with AS and NaCl at $S_c = 1.1$ %. The initial combustion size distribution at the start of the experiment and the modified CCN activation fractions of the aerosol mixtures are presented. The shape of the activation curve provides insight about the sizes of very hygroscopic and non-hygroscopic species. At $S_c = 1.1$ %, BC particles, with $\kappa = 0.001$, will not theoretically activate below 250 nm and the contribution of externally mixed BC in the size range shown does not contribute much (if any) CCN. The normalized size distribution data show that there are few BC-like particles at small sizes (< 50 nm), the majority of particles in this range are inorganic. Thus for both the AS and NaCl external mixtures, the activation diameters derived from a singular fit were consistent with the expected $d_{p50} < 50$ nm of the respective inorganic salts. Specifically at $S_c = 1.1$ %, AS and NaCl particles activated at 25 and 19 nm, respectively (congruent with theoretical dp50 at 24.8 and 19.0 nm) At the larger sizes ($>$ inorganic d_{p50}), the BC mixture concentration increased and the CCN / CN was depressed. The combustion aerosol alone is not CCN active at this S_c or size and the depressions are reflective of the non-hygroscopic combustion aerosol fraction in the aerosol sample. Notably, plateaus are dynamic. As the concentration of inorganic salts increases, the increased activated fraction is reflected in the CCN spectra; the plateau heights increase with increasing hygroscopic concentrations. In these particular externally mixed experiments, the initial CCN / CN plateau can be as large as 1, subsequently decrease, and then will likely increase to 1 after the BC critical diameters are reached. BC externally mixed with very hygroscopic material is more CCN active than the soot alone.

Succinic acid (SA) was mixed with combustion aerosol to investigate the external to internal mixing and transition of slightly hygroscopic organic with non-hygroscopic insoluble but wettable aerosols. The laboratory system mimics observed increases in secondary organic aerosol (SOA) mass fractions on combustion aerosols during atmospheric aging. The SA was introduced to the flow tube at various concentrations, followed by the combustion aerosol from the APG; under dry externally mixed conditions and bimodal size distribution peaks were observed (Fig. 9).

The normalized size distributions of the aerosol leaving the flow tube are presented. The initial soot size distribution is similar to those presented in Fig. 8. Assuming the first of the two peaks is SA, and the second is a mixture of the combustion aerosol and SA, the initial point of activation agrees with that of succinic acid where SA aerosols all activate. After a mobility diameter, $d_p > 50$ nm, the concentration of combustion aerosol in the mixture increases and

the CCN / CN ratio is < 0.2, indicative of a lower SA concentration relative to the non-activated BC concentration.

To induce internal mixing, active heating was again turned off for the atomized aerosol source. Again, internal mixing was promoted and the multiple activation curves converge into a single sigmoid for the BC and SA system. This is consistent with the AS–SA experiment and previous work that showed a strong influence of insoluble compounds on activation when internally mixed with a more soluble compound. (9) With continued mixing, a shift to larger activation diameters was observed towards the end of the experiment (scan 93) and there was a slight depression in the plateau of the CCN spectra.

The data suggest that only a small amount of soluble inorganic and organic material is required to make the soot more active than that observed alone, especially as the aerosol becomes more internally mixed.

5 Conclusions

Results confirm that the experimental CCN activation curves of aerosol provide insight into the type of mixing (e.g., internal vs. external) and the various levels of hygroscopicities that are chemically representative. Modifications in the concentrations of externally mixed non-hygroscopic aerosols are reflective of the CCN-activated concentrations. This is consistent with CCN spectra observed in ambient studies, which have attributed observations in CCN activation plateau heights less than one to the contributions of externally mixed and inactivated (typically non-hygroscopic black carbon) aerosols. This work adds to the existing body of CCN literature and demonstrates that the transition from external to internal mixtures can be mimicked in controlled laboratory experiments and observed in CCN data. If one accounts for multiple-sigmoid analysis in experimental CCN activation data, the CCN behavior of known hygroscopic compound mixtures (e.g., ammonium sulfate, sodium chloride, succinic acid) agrees well with traditional Köhler theory. However, more work is needed to explore mixtures of hygroscopic material particularly with wettable and non-hygroscopic aerosol. Here, as the non-hygroscopic combustion aerosol becomes internally mixed with the inorganic and organic material, the CCN activity of the combustion aerosol is modified. The data here, with recent publications (Altaf et al., 2018; Ye at al., 2016), suggest that aerosol water is a significant factor in promoting mixing and can be used to modify mixing states. To our knowledge, the technique provided here is the first to show aerosol population transitions from externally to internally mixed states in a laboratory environment and thus the technique can be applied to understand additional aerosol properties (e.g., optical, gas-phase uptake, subsaturated droplet growth) of known compounds that can modify particle mixing states. The aerosols studied here maintained an external mixture under dry con-
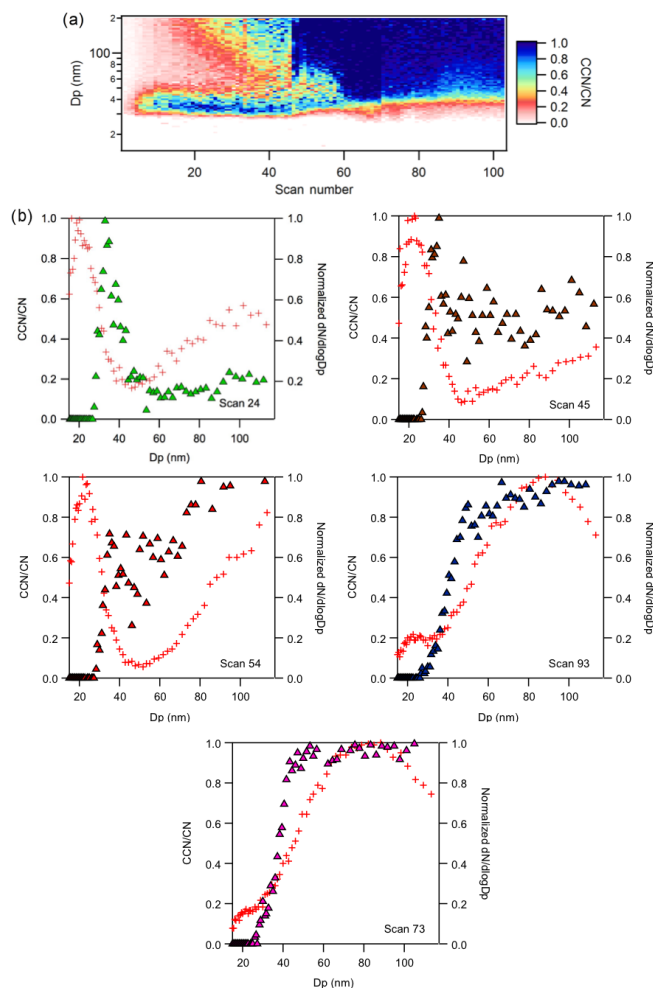
Figure 9. (a) Time series of CCN / CN activated fractions of succinic acid (SA) and combustion aerosol (BC) mixture in flow tube. (b) The CCN / CN activated fraction (closed triangles) of SA and BC mixtures for particle distribution scans 24, 45, 54, 73, and 94. Aerosol water is introduced at ∼ scan 70 to promote internal mixing. Cross symbols show the particle size distribution of mixed aerosol.

ditions; CCN activation curves plateaued and remained constant. However, turning off the heater promoted internal mixing and the activation curves were observed to converge. These experiments with known compounds validate that the aerosol mixing state can be observed in CCN activation data and can be applied to aerosol data sets to understand the extent of mixing. The results confirm that CCN counters and CCN analysis should be used in future studies to quantify the extent of mixing of ambient particles. The results are critical to understanding other factors important to the direct and indirect radiative contributions of atmospheric particles.

References

Abbatt, J. P. D., Broekhuizen, K., and Kumar, P. P.: Cloud condensation nucleus activity of internally mixed ammonium sulfate/organic acid aerosol particles, Atmos. Environ., 39, 4767–4778, 2005.

Almeida, G. P., Brito, J., Morales, C. A., Andrade, M. F., and Artaxo, P.: Measured and modelled cloud condensation nuclei (CCN) concentration in São Paulo, Brazil: the importance of aerosol size-resolved chemical composition on CCN con-

centration prediction, Atmos. Chem. Phys., 14, 7559–7572, https://doi.org/10.5194/acp-14-7559-2014, 2014.

Altaf, M. B. Dutcher, D. D. Raymond, T. M., and Freedman, M. A.: Effect of Particle Morphology on Cloud Condensation Nuclei Activity, ACS Earth and Space Chem., 8, 3613–3618, https://doi.org/10.1021/acsearthspacechem.7b00146 2018.

Asa-Awuku, A., Moore, R., Nenes, A., Bahreini, R., Brock, C. A., Middlebrook, A., Holloway, J., Ryerson, T., Jimenez, J., DeCarlo, P., Hecobian, A., Weber, R., Tanner, D., Stickel, R., and Huey L. G.: Airborne Cloud Condensation Nuclei Measurements during the 2006 Texas Air Quality Study, J. Geophys. Res., 116, D11201, https://doi.org/10.1029/2010JD014874 2011.

Bhattu, D. and Tripathi, S. N.: CCN closure study: Effects of aerosol chemical composition and mixing state, J. Geophys. Res.-Atmos., 120, 766–783, https://doi.org/10.1002/2014JD021978, 2015.

Bhattu, D., Tripathi, S. N., and Chakraborty, A.: Deriving aerosol hygroscopic mixing state from size-resolved CCN activity and HR-ToF-AMS measurements, Atmos. Environ., 142, 57–70, 2016.

Bilde, M. and Svenningsson, B.: CCN activation of slightly soluble organics: The importance of small amounts of inorganic salt and particle phase, Tellus, 56B, 128–134, 2004.

Bond, T. C., Doherty, S. J., Fahey, D. W., Forster, P. M., Berntsen, T., DeAngelo, B. J., Flanner, M. G., Ghan, S., Karcher, B., Koch, D., Kinne, S., Kondo, Y., Quinn, P. K., Sarofim, M. C., Schultz, M. G., Schulz, M., Venkataraman, C., Zhang, H., Zhang, S., Bellouin, N., Guttikunda, S. K., Hopke, P. K., Jacobson, M. Z., Kaiser, J. W., Klimont, Z., Lohmann, U., Schwarz, J. P., Shindell, D., Storelvmo, T., Warren, S. G., and Zender, C. S.: Bounding the role of black carbon in the climate system: A scientific assessment, J. Geophys. Res., 118, 5380–5552, 2013.

Bougiatioti, A., Nenes, A., Fountoukis, C., Kalivitis, N., Pandis, S. N., and Mihalopoulos, N.: Size-resolved CCN distributions and activation kinetics of aged continental and marine aerosol, Atmos. Chem. Phys., 11, 8791–8808, https://doi.org/10.5194/acp-11-8791-2011, 2011.

Broekhuizen, K., Kumar, P. P., and Abbatt, J. P. D.: Partially soluble organics as cloud condensation nuclei: Role of trace soluble and surface active species, Geophys. Res. Lett., 31, L01107, https://doi.org/10.1029/2003GL018203, 2004.

Cai, M., Tan, H., Chan, C. K., Qin, Y., Xu, H., Li, F., Schurman, M. I., Liu, L., and Zhao, J.: The size-resolved cloud condensation nuclei (CCN) activity and its prediction based on aerosol hygroscopicity and composition in the Pearl Delta River (PRD) region during wintertime 2014, Atmos. Chem. Phys., 18, 16419–16437, https://doi.org/10.5194/acp-18-16419-2018, 2018.

Che, H. C., Zhang, X. Y., Wang, Y. Q., Zhang, L., Shen, X. J., Zhang, Y. M., Ma, Q. L., Sun, J. Y., Zhang, Y. W., and Wang, T. T.: Characterization and parameterization of aerosol cloud condensation nuclei activation under different pollution conditions, Sci. Rep., 6, 24497, https://doi.org/10.1038/srep24497, 2016.

Chen, L., Li, Q., Wu, D., Sun, H., Wei, Y., Ding, X., Chen, H., Cheng, T., and Chen, J.: Size distribution and chemical composition of primary particles emitted during open biomass burning processes: Impacts on cloud condensation nuclei activation, Sci. Total Environ., 674, 179–188, 2019.

Ching, J., Riemer, N., and West, M.: Black carbon mixing state impacts on cloud microphysical properties: Effects of aerosol

plume and environmental conditions, J. Geophys. Res.,-Atmos, 121, 5990–6013, 2016.

Crosbie, E., Youn, J.-S., Balch, B., Wonaschütz, A., Shingler, T., Wang, Z., Conant, W. C., Betterton, E. A., and Sorooshian, A.: On the competition among aerosol number, size and composition in predicting CCN variability: a multi-annual field study in an urbanized desert, Atmos. Chem. Phys., 15, 6943–6958, https://doi.org/10.5194/acp-15-6943-2015, 2015.

Cruz, C. N. and Pandis, S. N.: The effect of organic coatings on the cloud condensation nuclei activation of inorganic atmospheric aerosol, J. Geophys. Res., 103, 13111–13123, 1998.

Cubison, M. J., Ervens, B., Feingold, G., Docherty, K. S., Ulbrich, I. M., Shields, L., Prather, K., Hering, S., and Jimenez, J. L.: The influence of chemical composition and mixing state of Los Angeles urban aerosol on CCN number and cloud properties, Atmos. Chem. Phys., 8, 5649–5667, https://doi.org/10.5194/acp-8-5649-2008, 2008.

DeCarlo, P. F., Kimmel, J. R., Trimborn, A., H., Northway, M. J., Jayne, J. T., Aiken, A. C., Gonin, M., Fuhrer, K., Horvath II, T., Docherty, K. S., Worsnop, D. R., and Jimenez, J. L.: Field Delopyable, High-Resolution, Time-of-Flight Aerosol Mass Spectrometer, Anal. Chem., 78, 8281–8289, 2006.

Durdina, L., Lobo, P., Trueblood, M.B., Black, E.A., Achterberg, S., Hagen, D., Brem, B.T., and Wang, J.: Response of black carbonmass instruments to mini-cast soot, Aerosol Sci. Technol., 50, 906–918, 2016.

Dusek, U., Frank, G. P., Hildebrandt, L., Curtius, J., Schneider, J., Walter, S., Chand, D., Drewnick, F., Hings, S., Jung, D., Borrmann, S., and Andreae, M. O.: Size matters more than chemistry for cloud-nucleating ability of aerosol particles, Science, 312, 1375–1378, 2006.

Ervens, B., Cubison, M., Andrews, E., Feingold, G., Ogren, J. A., Jimenez, J. L., DeCarlo, P., and Nenes, A.: Prediction of cloud condensation nucleus number concentration using measurements of aerosol size distributions and composition and light scattering enhancement due to humidity, J. Geophys. Res., 112, D10S32, https://doi.org/10.1029/2006JD007426, 2007.

Ervens, B., Cubison, M. J., Andrews, E., Feingold, G., Ogren, J. A., Jimenez, J. L., Quinn, P. K., Bates, T. S., Wang, J., Zhang, Q., Coe, H., Flynn, M., and Allan, J. D.: CCN predictions using simplified assumptions of organic aerosol composition and mixing state: a synthesis from six different locations, Atmos. Chem. Phys., 10, 4795–4807, https://doi.org/10.5194/acp-10-4795-2010, 2010.

Farmer, D. K., Cappa, C. D., and Kreidenweis, S.: Atmospheric processes and their controlling influence on cloud condensation nuclei activity, Chem. Rev., 115.10, 4199–4217, https://doi.org/10.1021/cr5006292, 2015.

Fofie, E. A., Donahue, N. M., and Asa-Awuku, A.: Cloud condensation nuclei activity and droplet formation of primary and secondary organic aerosol mixtures, Aerosol Sci. Technol., 52, 1–10, 2017.

Gibson, E. R., Gierlus, K. M., Hudson, P. K., and Grassian, V. H.: Generation of Internally Mixed Insoluble and Soluble Aerosol Particles to Investigate the Impact of Atmospheric Aging and Heterogeneous Processing on the CCN Activity of Mineral Dust Aerosol, Aerosol Sci. Technol., 41, 914–924, https://doi.org/10.1080/02786820701557222, 2007.

Hameri, K., Charlson, R., and Hansson, H. C.: Hygroscopic Properties of Mixed Ammonium Sulfate and Carboxylic Acids Particles, AICHE J., 48, 1309–1316, 2002.

Henning, S., Rosenørn, T., D'Anna, B., Gola, A. A., Svenningsson, B., and Bilde, M.: Cloud droplet activation and surface tension of mixtures of slightly soluble organics and inorganic salt, Atmos. Chem. Phys., 5, 575–582, https://doi.org/10.5194/acp-5-575-2005, 2005.

Jurányi, Z., Tritscher, T., Gysel, M., Laborde, M., Gomes, L., Roberts, G., Baltensperger, U., and Weingartner, E.: Hygroscopic mixing state of urban aerosol derived from size-resolved cloud condensation nuclei measurements during the MEGAPOLI campaign in Paris, Atmos. Chem. Phys., 13, 6431–6446, https://doi.org/10.5194/acp-13-6431-2013, 2013.

Kim, N., Park, M., Yum, S. S., Park, J. S., Shin, H. J., and Ahn, J. Y.: Impact of urban aerosol properties on cloud condensation nuclei (CCN) activity during the KORUS-AQ field campaign, Atmos. Environ., 185, 221–236, 2018.

King, S. M., Rosenoern, T., Shilling, J. E., Chen, Q., and Martin, S. T.: Cloud condensation nucleus activity of secondary organic aerosol particles mixed with sulfate, Geophys. Res. Lett., 34, L24806, https://doi.org/10.1029/2007GL030390, 2007.

Koehler, K. A., DeMott, P. J., Kreidenweis, S. M., Popovicheva, O. B., Petters, M. D., Carrico, C. M., Kireeva, E. D., Khokhlova, T. D., and Shonija, N. K.: Cloud condensation nuclei and ice nucleation activity of hydrophobic and hydrophilic soot particles, Phys. Chem. Chem. Phys., 11, 7906–7920, 2009.

Kuwata, M. and Kondo, Y.: Dependence of size-resolved CCN spectra on the mixing state of nonvolatile cores observed in Tokyo, J. Geophys. Res., 113, D19202, https://doi.org/10.1029/2007JD009761, 2008.

Lammel, G. and Novakov, T.: Water Nucleation Properties of Carbon-Black and Diesel Soot Particles, Atmos. Environ., 29, 813–823, 1995.

Lance, S., Raatikainen, T., Onasch, T. B., Worsnop, D. R., Yu, X.-Y., Alexander, M. L., Stolzenburg, M. R., McMurry, P. H., Smith, J. N., and Nenes, A.: Aerosol mixing state, hygroscopic growth and cloud activation efficiency during MIRAGE 2006, Atmos. Chem. Phys., 13, 5049–5062, https://doi.org/10.5194/acp-13-5049-2013, 2013.

Liu, D., Allan, J., Whitehead, J., Young, D., Flynn, M., Coe, H., McFiggans, G., Fleming, Z. L., and Bandy, B.: Ambient black carbon particle hygroscopic properties controlled by mixing state and composition, Atmos. Chem. Phys., 13, 2015–2029, https://doi.org/10.5194/acp-13-2015-2013, 2013.

Mahish, M., Jefferson, A., and Collins, D. R.: Influence of Common Assumptions Regarding Aerosol Composition and Mixing State on Predicted CCN Concentration, Atmosphere, 9, 54, 2018.

Mallet, M. D., Cravigan, L. T., Milic, A., Alroe, J., Ristovski, Z. D., Ward, J., Keywood, M., Williams, L. R., Selleck, P., and Miljevic, B.: Composition, size and cloud condensation nuclei activity of biomass burning aerosol from northern Australian savannah fires, Atmos. Chem. Phys., 17, 3605–3617, https://doi.org/10.5194/acp-17-3605-2017, 2017.

Mamakos, A., Khalek, I., Giannelli, R., and Spears, M.: Characterization of Combustion Aerosol Produced by a Mini-CAST and Treated in a Catalytic Stripper, Aerosol Sci. Technol., 47, 927–936, https://doi.org/10.1080/02786826.2013.802762, 2013.

Maricq, M. M. and Matti Maricq, M.: Examining the Relationship Between Black Carbon and Soot in Flames and Engine Exhaust, Aerosol Sci. Technol., 48, 620–629, https://doi.org/10.1080/02786826.2014.904961, 2014.

McMeeking, G. R., Good, N., Petters, M. D., McFiggans, G., and Coe, H.: Influences on the fraction of hydrophobic and hydrophilic black carbon in the atmosphere, Atmos. Chem. Phys., 11, 5099–5112, https://doi.org/10.5194/acp-11-5099-2011, 2011.

Meng, J. W., Yeung, M. C., Li, Y. J., Lee, B. Y. L., and Chan, C. K.: Size-resolved cloud condensation nuclei (CCN) activity and closure analysis at the HKUST Supersite in Hong Kong, Atmos. Chem. Phys., 14, 10267–10282, https://doi.org/10.5194/acp-14-10267-2014, 2014.

Moore, R. H., Nenes, A., and Medina, J.: Scanning Mobility CCN Analysis – A Method for Fast Measurements of Size-Resolved CCN Distributions and Activation Kinetics, Aerosol Sci. Technol., 44, 861–871, 2010.

Moore, R. H., Cerully, K., Bahreini, R., Brock, C. A., Middlebrook, A. M., and Nenes, A.: Hygroscopicity and composition of California CCN during summer 2010, J. Geophys. Res., 117, D00V12, https://doi.org/10.1029/2011JD017352, 2012.

Moore, R. H., Ziemba, L. D., Dutcher, D., Beyersdorf, A. J., Chan, K., Crumeyrolle, S., Raymond, T. M., Thornhill, K. L., Winstead, E. L., and Anderson, B. E.: Mapping the Operation of the Miniature Combustion Aerosol Standard (Mini-CAST) Soot Generator, Aerosol Sci.Technol., 48, 467–479, https://doi.org/10.1080/02786826.2014.890694, 2014.

Padró, L. T., Asa-Awuku, A., Morrison, R., and Nenes, A.: Inferring thermodynamic properties from CCN activation experiments: single-component and binary aerosols, Atmos. Chem. Phys., 7, 5263–5274, https://doi.org/10.5194/acp-7-5263-2007, 2007.

Padró, L. T., Moore, R. H., Zhang, X., Rastogi, N., Weber, R. J., and Nenes, A.: Mixing state and compositional effects on CCN activity and droplet growth kinetics of size-resolved CCN in an urban environment, Atmos. Chem. Phys., 12, 10239–10255, https://doi.org/10.5194/acp-12-10239-2012, 2012.

Paramonov, M., Aalto, P. P., Asmi, A., Prisle, N., Kerminen, V.-M., Kulmala, M., and Petäjä, T.: The analysis of size-segregated cloud condensation nuclei counter (CCNC) data and its implications for cloud droplet activation, Atmos. Chem. Phys., 13, 10285–10301, https://doi.org/10.5194/acp-13-10285-2013, 2013.

Petters, M. D. and Kreidenweis, S. M.: A single parameter representation of hygroscopic growth and cloud condensation nucleus activity, Atmos. Chem. Phys., 7, 1961–1971, https://doi.org/10.5194/acp-7-1961-2007, 2007.

Petters, M. D. and Kreidenweis, S. M.: A single parameter representation of hygroscopic growth and cloud condensation nucleus activity – Part 2: Including solubility, Atmos. Chem. Phys., 8, 6273–6279, https://doi.org/10.5194/acp-8-6273-2008, 2008.

Pinho, C. E. L., João M P, Ferreira, V., Pilão, R. and Pinho, C.: Influence of Burner Geometry on Flame Characteristics of Propane-Air Mixture: Experimental and Numerical Studies, Defect and Diffusion Forum, 273–276, 162–167, 2008.

Pruppacher, H. R. and Klett, J. D.: Microphysics of Clouds and Precipitation, 954, Kluwar Acad., Norwell Mass., 1997.

Riemer, N., Ault, A. P., West, M., Craig, R. L., and Curtis, J. H.: Aerosol Mixing State: Measurements, Modeling, and Impacts, Rev. Geophys., 57, 187–249, https://doi.org/10.1029/2018rg000615, 2019.

Roberts, G. C. and Nenes, A.: A Continuous-Flow Streamwise Thermal-Gradient CCN Chamber for Atmospheric Measurements, Aerosol Sci. Technol., 35, 206–2011, https://doi.org/10.1080/027868290913988, 2005.

Rojas, L., Peraza, A., and Ruette, F.: Aging Oxidation Reactions on Atmospheric Black Carbon by OH Radicals. A Theoretical Modeling Study, J. Phys. Chem. A, 119, 13038–13047, 2015.

Rose, D., Gunthe, S. S., Mikhailov, E., Frank, G. P., Dusek, U., Andreae, M. O., and Pöschl, U.: Calibration and measurement uncertainties of a continuous-flow cloud condensation nuclei counter (DMT-CCNC): CCN activation of ammonium sulfate and sodium chloride aerosol particles in theory and experiment, Atmos. Chem. Phys., 8, 1153–1179, https://doi.org/10.5194/acp-8-1153-2008, 2008.

Sánchez Gácita, M., Longo, K. M., Freire, J. L. M., Freitas, S. R., and Martin, S. T.: Impact of mixing state and hygroscopicity on CCN activity of biomass burning aerosol in Amazonia, Atmos. Chem. Phys., 17, 2373–2392, https://doi.org/10.5194/acp-17-2373-2017, 2017.

Schill, S. R., Collins, D. B., Lee, C., Morris, H. S., Novak, G. A., Prather, K. A., and Bertram, T. H.: The Impact of Aerosol Particle Mixing State on the Hygroscopicity of Sea Spray Aerosol, ACS Central Science, 1, 132–141, https://doi.org/10.1021/acscentsci.5b00174, 2015.

Schmale, J., Henning, S., Decesari, S., Henzing, B., Keskinen, H., Sellegri, K., Ovadnevaite, J., Pöhlker, M. L., Brito, J., Bougiatioti, A., Kristensson, A., Kalivitis, N., Stavroulas, I., Carbone, S., Jefferson, A., Park, M., Schlag, P., Iwamoto, Y., Aalto, P., Äijälä, M., Bukowiecki, N., Ehn, M., Frank, G., Fröhlich, R., Frumau, A., Herrmann, E., Herrmann, H., Holzinger, R., Kos, G., Kulmala, M., Mihalopoulos, N., Nenes, A., O'Dowd, C., Petäjä, T., Picard, D., Pöhlker, C., Pöschl, U., Poulain, L., Prévôt, A. S. H., Swietlicki, E., Andreae, M. O., Artaxo, P., Wiedensohler, A., Ogren, J., Matsuki, A., Yum, S. S., Stratmann, F., Baltensperger, U., and Gysel, M.: Long-term cloud condensation nuclei number concentration, particle number size distribution and chemical composition measurements at regionally representative observatories, Atmos. Chem. Phys., 18, 2853–2881, https://doi.org/10.5194/acp-18-2853-2018, 2018.

Seinfeld, J. H. and Pandis, S. N.: Atmospheric Chemistry and Physics, John Wiley, New York, 1998.

Seong, H. J. and Boehman, A. L.: Studies of soot oxidative reactivity using a diffusion flame burner, Combust. Flame, 159, 1864–1875, https://doi.org/10.1016/j.combustflame.2012.01.009, 2012.

Shulman, M. L., Jacobson, M. C., Charlson, R. J., Synovec, R. E., and Young, T. E.: Dissolution behavior and surface tension effects of organic compounds in nucleating cloud droplets, Geophys. Res. Lett., 23, 277–280, 1996.

Spracklen, D. V., Carslaw, K. S., Pöschl, U., Rap, A., and Forster, P. M.: Global cloud condensation nuclei influenced by carbonaceous combustion aerosol, Atmos. Chem. Phys., 11, 9067–9087, https://doi.org/10.5194/acp-11-9067-2011, 2011.

Stevens, R. and Dastoor, A.: A Review of the Representation of Aerosol Mixing State in Atmospheric Models, Atmosphere, 10, 168, https://doi.org/10.3390/atmos10040168, 2019.

Su, H., Rose, D., Cheng, Y. F., Gunthe, S. S., Massling, A., Stock, M., Wiedensohler, A., Andreae, M. O., and Pöschl, U.: Hygroscopicity distribution concept for measurement data analysis and modeling of aerosol particle mixing state with regard to hygroscopic growth and CCN activation, Atmos. Chem. Phys., 10, 7489–7503, https://doi.org/10.5194/acp-10-7489-2010, 2010.

Sullivan, R. C., Moore, M. J. K., Petters, M. D., Kreidenweis, S. M., Roberts, G. C., and Prather, K. A.: Effect of chemical mixing state on the hygroscopicity and cloud nucleation properties of calcium mineral dust particles, Atmos. Chem. Phys., 9, 3303–3316, https://doi.org/10.5194/acp-9-3303-2009, 2009.

Svenningsson, B., Rissler, J., Swietlicki, E., Mircea, M., Bilde, M., Facchini, M. C., Decesari, S., Fuzzi, S., Zhou, J., Mønster, J., and Rosenørn, T.: Hygroscopic growth and critical supersaturations for mixed aerosol particles of inorganic and organic compounds of atmospheric relevance, Atmos. Chem. Phys., 6, 1937–1952, https://doi.org/10.5194/acp-6-1937-2006, 2006.

Vu, D., Short, D., Karavalakis, G., Durbin, T. D., and Asa-Awuku, A.: Integrating cloud condensation nuclei predictions with fast time resolved aerosol instrumentation to determine the hygroscopic properties of emissions over transient drive cycles, Aerosol Sci. Technol., 49, 1149–1159, 2015.

Wang, J., Cubison, M. J., Aiken, A. C., Jimenez, J. L., and Collins, D. R.: The importance of aerosol mixing state and size-resolved composition on CCN concentration and the variation of the importance with atmospheric aging of aerosols, Atmos. Chem. Phys., 10, 7267–7283, https://doi.org/10.5194/acp-10-7267-2010, 2010.

Weingartner, E., Burtscher, H., and Baltensperger, U.: Hygroscopic properties of carbon and diesel soot particles, Atmos. Environ., 31, 2311–2327, https://doi.org/10.1016/s1352-2310(97)00023-x, 1997.

Wex, H., McFiggans, G., Henning, S., and Stratmann, F.: Influence of the external mixing state of atmospheric aerosol on derived CCN number concentrations, Geophys. Res. Lett., 37, L10805, https://doi.org/10.1029/2010GL043337, 2010.

Winkler, P.: The growth of atmospheric aerosol particles as a function of the relative humidity – II. An improved concept of mixed nuclei, J. Aerosol Sci., 4, 373–387, 1973.

Ye, Q., Robinson, E. S., Ding, X., Ye, P., Sullivan, R., and Robinson, N.: Mixing of secondary organic aerosols versus relative humidity, P. Natl. Acad. Sci. USA, 113, 12649–12654, 2016.

Zaveri, R. A., Barnard, J. C., Easter, R. C., Riemer, N., and West, M.: Particle-resolved simulation of aerosol size, composition, mixing state, and the associated optical and cloud condensation nuclei activation properties in an evolving urban plume, J. Geophys. Res.-Atmos., 115, D17210, https://doi.org/10.1029/2009JD013616, 2010.